# BMP Gene-immobilization to Dental Implants Enhances Bone Regeneration

*Shogo Maekawa, Young-Dan Cho, Frederic Kauffmann, Yao Yao, James V. Sugai, Xiaoyang Zhong, Caroline Schmiedeler, Nitin Kinra, Alyssa Moy, Lena Larsson, Joerg Lahann, William V. Giannobile**

S. Maekawa, W. V. Giannobile

Department of Oral Medicine, Infection, and Immunity, Harvard School of Dental Medicine, 188 Longwood Avenue, Boston, MA 02115, USA.

Email: William_Giannobile@hsdm.harvard.edu

S. Maekawa

Department of Periodontology, Graduate School of Medical and Dental Sciences, Tokyo Medical and Dental University, Tokyo, 113-5810, Japan

Y. D. Cho

Department of Periodontology, School of Dentistry and Dental Research Institute, Seoul National University and Seoul National University Dental Hospital. Yeongeon-dong, Jongno-gu, 03080, Seoul, Korea

F. Kauffmann



This is the author manuscript accepted for publication and has undergone full peer review but has not been through the copyediting, typesetting, pagination and proofreading process, which may lead to differences between this version and the Version of Record. Please cite this article as doi: 10.1002/admi.202200531.

Department of Oral and Craniomaxillofacial Surgery, Center for Dental Medicine, University Medical Center Freiburg, Freiburg im Breisgau, 79110, Germany

Y. Yao, J. V. Sugai, C. Schmiedeler, N. Kinra, A. Moy

Department of Periodontics and Oral Medicine, University of Michigan School of Dentistry, Ann Arbor, MI 48109, USA

Y. Yao, J. V. Sugai, X Zhong, J. Lahann

Biointerfaces Institute, University of Michigan, Ann Arbor, MI 48109, USA

X. Zhong, J. Lahann

Department of Materials Science and Engineering, University of Michigan, Ann Arbor, MI 48109, USA

L. Larsson

Department of Periodontology, Institute of Odontology, University of Gothenburg, Gothenburg, 41390, Sweden

Keywords: Bone regeneration, Chemical Vapor Deposition, Gene Delivery, Implant, BMP-7



**Abstract**

For individuals who have experienced tooth loss, dental implants are an important treatment option for oral reconstruction. For these patients, alveolar bone augmentation and acceleration of osseointegration optimizes implant stability. Traditional oral surgery often requires

invasive procedures, which can result in prolonged treatment time and associated morbidity. We have previously shown that chemical vapor deposition (CVD) polymerization of functionalized [2.2] paracyclophanes can be used to anchor gene encoding vectors onto biomaterial surfaces and local delivery of a bone morphogenetic protein (BMP)-encoding vector can increase alveolar bone volume and density in vivo. This study is the first to combine the use of CVD technology and BMP gene delivery on titanium for the promotion of bone regeneration and bone to implant contact in vivo. BMP-7 tethered to titanium surface enhances osteoblast cell differentiation and alkaline phosphatase activity in vitro and increases alveolar bone regeneration and % bone to implant contact similar to using high doses of exogenously applied BMP-7 in vivo. The use of this innovative gene delivery strategy on implant surfaces offers an alternative treatment option for targeted alveolar bone reconstruction.

## 1. Introduction

The discovery and development of titanium dental implants has led to major improvements in the rehabilitation of patients experiencing tooth loss[1]. At present, implant placement is one of the most common treatments in dentistry for restoring occlusal function, esthetics, and phonetics in response to tooth loss due to disease, injury, or congenital malformations[2]. One of the most common causes of tooth loss is periodontitis, a chronic inflammatory disease leading to subsequent loss of tissue attachment and alveolar bone supporting teeth. In recent decades, the global life expectancy has increased, and with it, the prevalence and the incidence of periodontal disease[3]. Thus, placement of implants in these patients presents a challenge for clinicians, highlighting the necessity to continue the discovery of innovative treatment options in order to provide sufficient bone volume and bone quality for more successful clinical outcomes.

At present, a variety of bioengineering approaches are clinically available, which have demonstrated promising results to locally stimulate bone regeneration and bone augmentation at the site of bone loss. The use of growth factors such as bone morphogenetic proteins (BMPs) have been at the forefront as regenerative treatments[4]. The use of targeted and site-specific approaches to stimulate local bone formation offers significant potential to target growth factors to the dental implant site. Local delivery of BMPs promote osteogenesis and accelerates implant osseointegration[5]. Yet, there remains a need for improving local growth factor target delivery to maintain and release growth factors in a more controlled and temporal manner.

We have previously utilized a unique method, known as chemical vapor deposition (CVD) polymerization, to bind gene therapy vectors directly onto the surfaces of biomaterials, such as polylactic-co-glycolic acid (PLGA), polycaprolactone (PCL), and titanium (Ti). Gene delivery using CVD on these biomaterials has been shown to establish a more prolonged and sustained factor delivery than traditional, recombinant protein delivery[6]. While systemically delivered adenoviral vectors have been shown to be captured by liver and lung[7], the use of CVD may overcome the safety concern associated with systemic distribution of unbound gene therapy vectors due to specific targeting and release onto biomaterial surfaces[6].

BMP-encoding gene therapy vectors extend the delivery period of growth factors and reduce the functional dose required to local defects[8] while other studies have demonstrated the safety and efficacy of using gene therapy vectors for oral tissue regeneration in vivo[9]. We propose using this novel method of CVD as a biomaterial surface modification technology to tether BMP-7 vectors onto titanium surfaces to increase local bone regeneration and osseointegration at implant defect sites.

## 2. Results and Discussion

### 2.1. Immobilization of Ad-BMP7 on titanium using CVD produces bioactive BMP-7 protein and promotes favorable cellular activities including cell adhesion and proliferation

We have previously developed and applied CVD technology to tether adenoviral vectors onto the surface of different biomaterials[6,10]. In this study, we applied CVD polymerization of functionalized [2.2]paracyclophanes to immobilize Ad-BMP7 onto Ti discs (**Figure 1**A). Briefly, Ad-BMP7 was tethered onto Ti discs following the binding of an anti-adenovirus antibody to the pentafluorophenol (PFP)-ester groups on the polymer coating. The active, functional group of the polymer, PFP ester, binds to the amino groups of the antibody via forming amide bonds with the amino groups of the antibody. Based on our preliminary work, the polymer adheres strongly to the surface[11]. The PFP group is removed upon incubation and binding of the antibody. After immobilization, the polymer is not biodegradeable meaning it is stable, and has been tested and is not bioreactive or cytotoxic. Based on the studies published by Hao et al. and Zhang et al.[6,12], this polymer layer can capture anti-adenovirus antibody via covalent immobilization on the $TiO_2$ surface. In the process, the reactive ester layer is replaced by a monolayer of antibodies as shown in Figure 1, and is thus not cytotoxic. We do not expect any remaining PFP ester groups on the titanium discs or implants after successful immobilization due to their strong hydrolytic lability. This functional polymer layer was proved to be stable with strong binding efficiency when incubated in physiological medium and there is no activation necessary. Binding efficacy was nearly 100% within a wide range from $10^8$ to $10^{11}$ particle number (PN). We used an antibody concentration above saturation (10 µg/ml) so that all functional groups are bound with antibody or blocked.

The attachment of adenovirus onto Ti has previously been demonstrated by our group using scanning electron microscopy[6]. In this publication the number of virus particles on the titanium surface was measured using six independent ROIs of 101,4 µm $^2$ each. Virus particles attached to the titanium surface for $10^{11}$ and $10^{12}$ PN were approximately 10 and 100 virus particles/ROI, respectively. To confirm that cells that could be transduced by an immobilized adenovirus vector, an Ad-Green Fluorescent Protein (GFP) vector, was tethered onto the CVD-treated titanium surface and using fluorescence microscopy, verified that the primary human cells coming into contact with the implant were transduced by the Ad-GFP vector and expressed the encoded GFP gene. (Supplementary Figure S1 and S2).

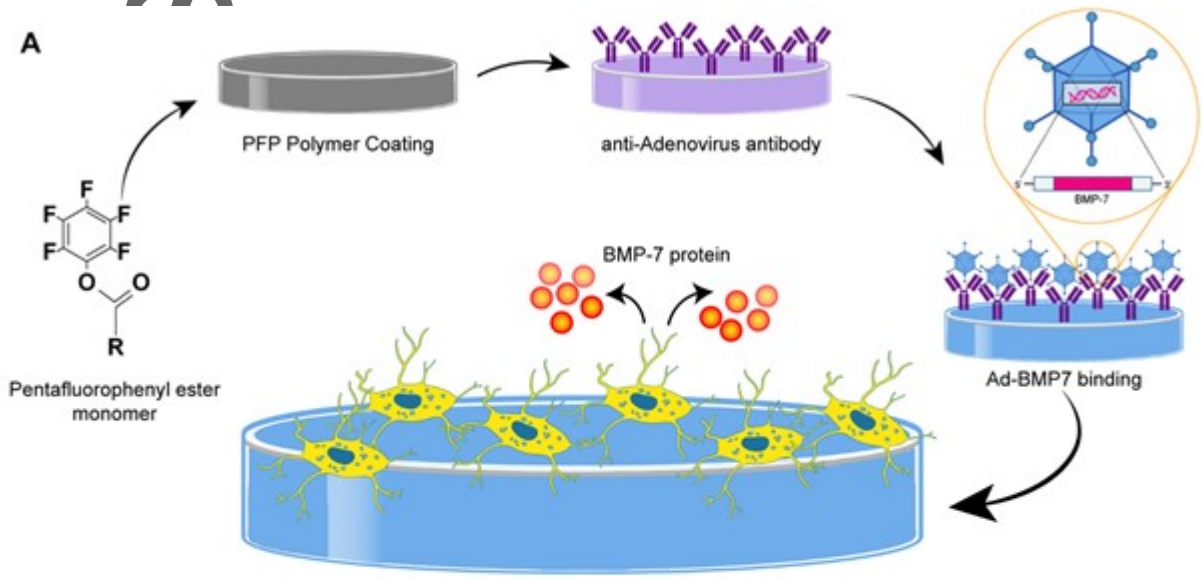


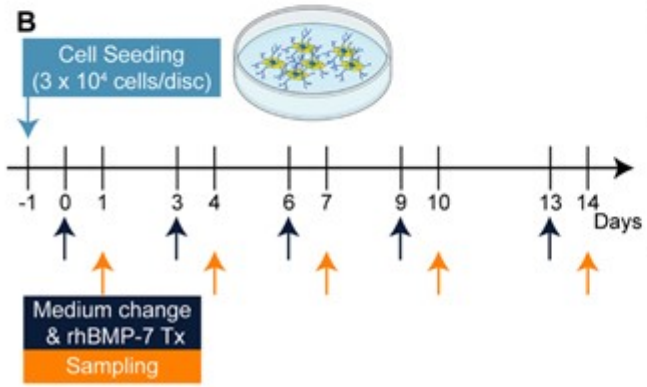


C

| Experimental/Control Type | Treatment |
|---|---|
| Negative Control | no treatment |
| Sham Control | CVD + Ad-empty |
| Low dose of Ad-BMP7 | CVD + Ad-BMP7 ($PN10^{11}$) |
| High dose of Ad-BMP7 | CVD + Ad-BMP7 ($PN10^{12}$) |
| Positive Control | rhBMP-7 (50ng/ml) |

**Figure 1. Experimental design of the in vitro study.**

A. Schematic rendering of the chemical vapor deposition (CVD) polymerization depicting sublimation of the pentafluorophenol (PFP) ester precursor, which forms a 17.3 ± 0.2 (mean ± SD) nm polymer coating onto the titanium surfaces. Following incubation with an anti-adenovirus antibody (10 µg/ml) and BMP-7-encoding adenovirus ($10^{11}$ PN), MC3T3-E1 cells ($3x10^4$ cells/disc) were added and incubated. B. The experimental timeline showing the timepoints for osteoblast-induction media changes and collection of the supernatant samples for subsequent analysis. c. Table showing the experimental and control treatment groups.

We first hypothesized that BMP7 gene delivery using CVD technology could transduce osteoblasts (OBs) and increase the differentiation and mineralization in vitro and subsequently improve dental implant osseointegration and bone regeneration in vivo. To test our hypothesis, we performed in vitro experiments using MC3T3-E1 pre-OBs seeded onto both CVD-treated and untreated Ti discs. Cells and supernatant cell culture media were harvested at each time point (Figure 1B), and five groups were tested (Figure 1C). On day 1 (Figure 1B), confocal laser scanning microscopy (CLSM) analysis showed that the cells adhered to the discs with no difference in cell adhesion observed between the no treatment and rhBMP-7 groups (**Figure 2**A). Regarding cell morphology, cells that were attached to the CVD-coated surface for both the CVD + Empty vector ($10^{11}$ PN/ml) and CVD+Ad-BMP7 ($10^{11}$, $10^{12}$ PN/ml) groups exhibited a more elongated and thin cytoskeletal appearance compared to cells attached to the untreated discs. Also, there appeared to be less cells attached when cultured on the CVD-treated discs compared to those grown on non-CVD discs (no treatment and rhBMP-7). Next, to quantify the concentration of soluble BMP-7 protein in the supernatants, which was produced from cells induced with Ad-BMP7, an enzyme-linked immunosorbent assay (ELISA) was performed (Figure 2B). Two concentrations of Ad-BMP7, $10^{11}$ and $10^{12}$ PN, were used and the data revealed that both PN concentrations of Ad-BMP7 produced a robust amount of BMP-7 protein over 14 days, forming a peak at day 7 (Figure 2B). In addition, our previous study showed the protein production and cell proliferation using Ad-PDGF and CVD was similar to rhPDGF-BB (50 ng/ml)[6]. Based on this result, the concentration of rhBMP-7 (positive

control) used for subsequent assays was selected at 50 ng/ml (Figure 1C). Finally, results from an MTT assay showed that metabolic activity increased over time with a similar proliferation profile for all groups. The cell numbers after day 1 of the non-CVD group were higher than that of the CVD group (Figure 2C), which was consistent with the CLSM image shown in Figure 2A.

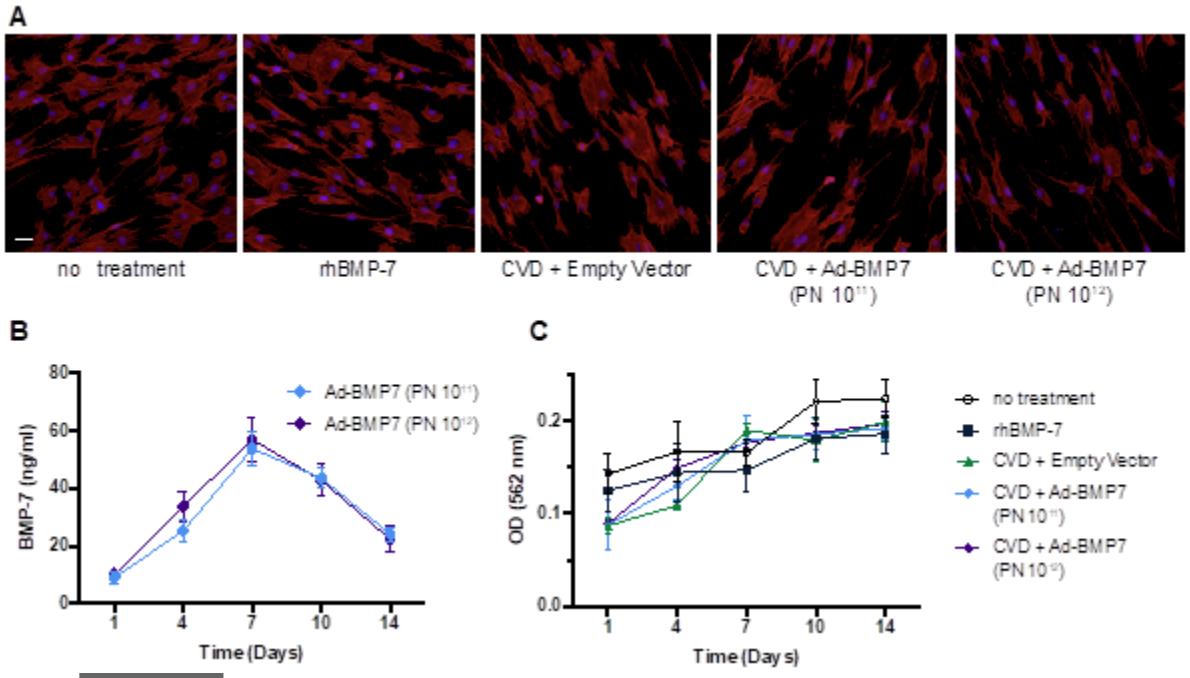


**Figure 2. Analysis of the MC3T3-E1 cellular phenotypic changes, BMP-7 protein production, and metabolic activity following incubation with Ad-BMP7-immobilized onto CVD coated titanium (Ti) discs.**

A. Confocal microscopy images of DAPI (blue)- and Phalloidin (red)-stained osteoblasts on the surface of the Ti discs at Day 1. Scale bar = 50 µm. B. ELISA assay measuring BMP-7 protein produced by MC3T3-E1 cells incubated with Ti discs over 14 days. C. MTT assay measuring the metabolic activity of osteoblast cells up to 14 days after incubation with Ti discs treated as shown. Three Discs/group were used and all samples were run in duplicate, and the data are expressed as mean ± SD of three independent experiments. Student t-test and One-way ANOVA with Tukey's post-hoc test were used. There was no significant difference among the groups regarding both BMP-7 production and cellular proliferation.

**2.2. Ad-BMP7 has a similar or higher osteogenic potential in vitro compared to rhBMP-7 treatment**

Osteoblast lineage progenitor cells undergo three differentiation phases: (1) cell proliferation, (2) extracellular matrix (ECM) secretion and maturation, and (3) matrix mineralization[13]. Following the initial active cell proliferation phase, immature OBs differentiate into mature OBs secreting both type 1 collagen, a major component of ECM, and ALP for ECM maturation[14]. Upon completion of ECM maturation, matrix mineralization occurs, expressing various osteoblastogenic markers including osteocalcin (OCN), osteopontin (OPN), and bone sialoprotein (BSP), with continued expression of Type I collagen and ALP[15]. RUNX2 is a master transcription factor stimulating expression of bone marker genes in osteoblastogenesis. The level of RUNX2 expression peaks between the immature and mature OB stages[16]. We then evaluated the osteoblastogenesis of MC3T3-E1 pre-OBs in each group. Cells were seeded onto Ti discs and OB differentiation was induced for 14 days using osteogenic media (Figure 1B). Quantitative real-time PCR was performed to measure the expression of representative bone marker genes; *Type 1 collagen*, *Runx2*, *Alp*, and *Ocn* (**Figure 3**A). Our data showed that *Type I collagen* was primarily expressed in the early stages around day 4, and *Runx2*, *Alp*, and *Ocn* expression increased sequentially until day 14 of cell culture (Figure 3A). Based on previous research studies, we concluded that OB differentiation followed a traditional pathway/timeline of osteoblastogenesis. Although all groups showed a similar OB differentiation pattern, the degree of differentiation varied slightly among the groups. The no treatment and CVD + empty vector groups yielded a lower differentiation capacity than the groups with BMP7 (rhBMP-7, Ad-BMP7). Notably, the CVD + Ad-BMP7 groups ($10^{11}$ and $10^{12}$) exhibited equivalent or slightly higher osteogenic potential compared to that of rhBMP-7. In addition, an ALP activity assay was performed to verify the osteogenic effects of Ad-BMP7, and indicated that both $10^{11}$ and $10^{12}$ PN resulted in greater ALP activity than rhBMP-7 treatment, with the CVD + Ad-BMP7 ($PN10^{11}$) group showing a significant peak of ALP protein production at day 10 (Figure 3B). Since gene expression alone does not simply explain bone regeneration, it was specifically concluded with the in vivo portion of the study. Based on this confirmation of the osteogenic potential of tethering Ad-BMP7 on Ti discs in vitro, we hypothesized

that immobilizing Ad-BMP7 onto titanium oral implants would enhance alveolar bone regeneration in vivo and improve osseointegration of the implants.

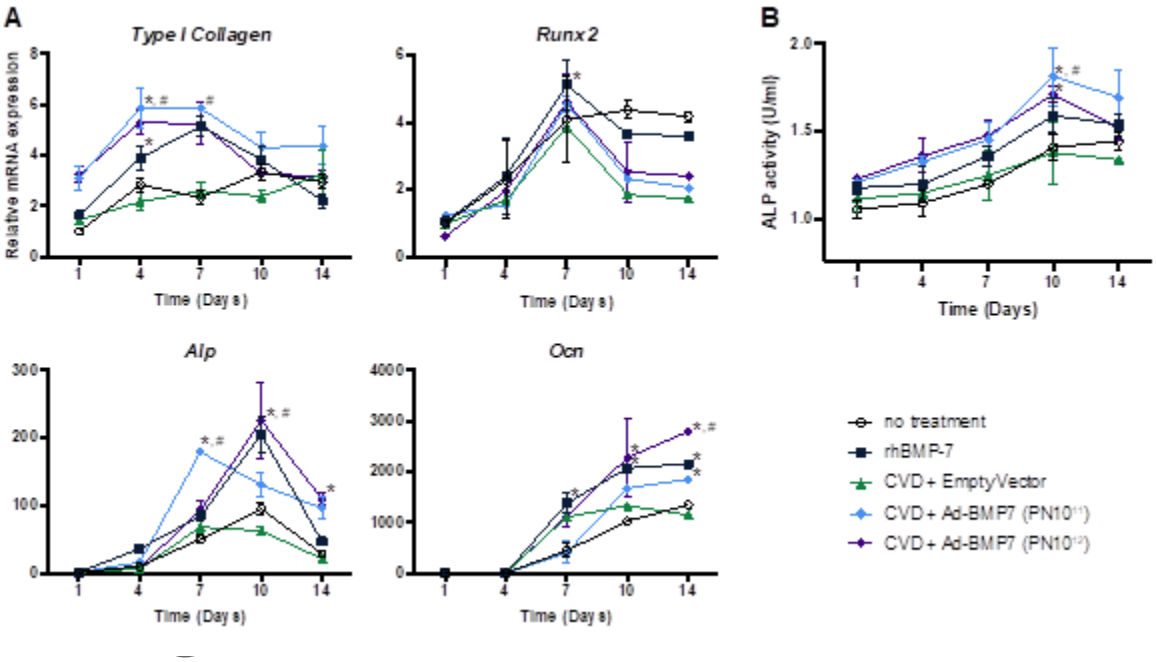


**Figure 3. Results from the in vitro study measuring gene and protein expression from MC3T3-E1 cells incubated on the CVD-treated Ti discs**.

A. Real-time PCR measurements of mRNA expression levels for Type I collagen, Runx2, alkaline phosphatase (ALP), and osteocalcin (OCN). B. Alkaline phosphatase protein expression level over 14 d of incubation of MC3T3-E1 cells with Ti discs, treated as shown. Three Discs/group were used and all samples were run in duplicate, and the data are expressed as mean ± SD of three independent experiments. One-way ANOVA with Tukey's post-hoc test was used. * $p < 0.05$ compared to no treatment and # $p < 0.05$ compared to rhBMP-7 on each corresponding day.

### 2.3. Ad-BMP7 enhanced bone regeneration and bone mineral density around implants in vivo

In order to examine the in vivo effects of using CVD coating and gene delivery on titanium implants for improved bone to implant contact (BIC) and bone regeneration, we performed implant surgical procedures in Sprague-Dawley rats. To standardize the placement of the implants, we created standardized bone defects using a customized implant step drill and titanium press-fit mini implants (**Figure 4**A). The implant surgeries were performed by an experienced surgeon (FK) according to an established protocol (Figure 4B-D). The outline of the complete surgical procedure, including molar extraction and socket healing, is shown in Figure 4C.

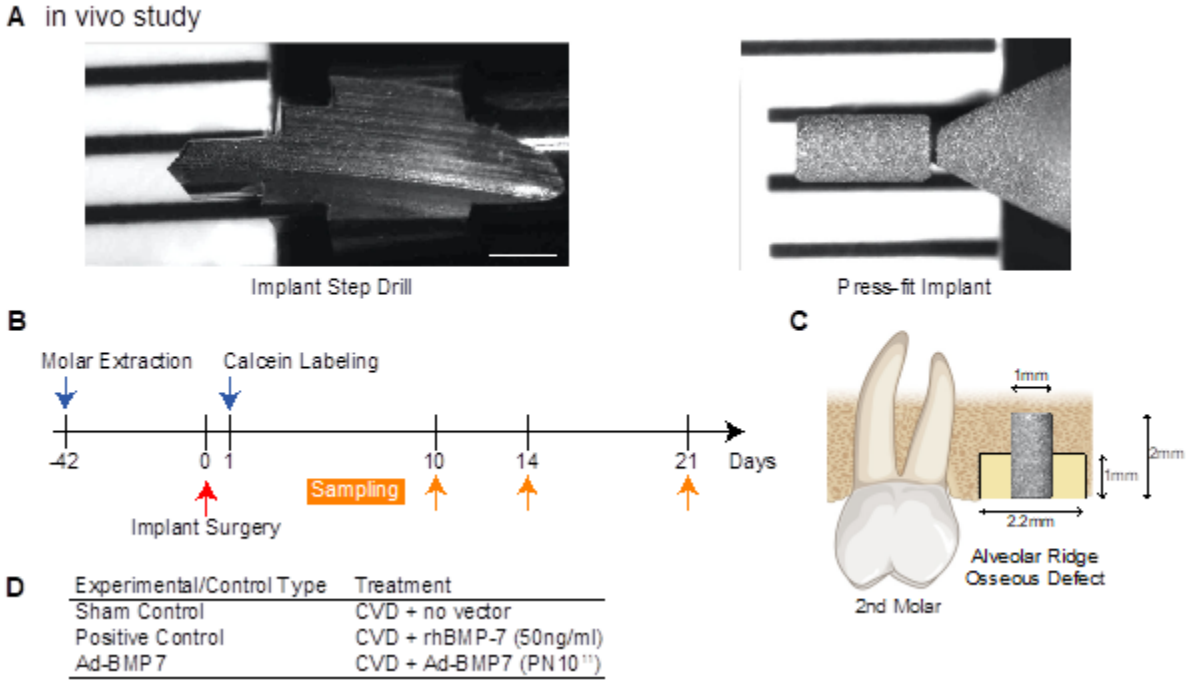


D

| Experimental/Control Type | Treatment |
|---|---|
| Sham Control | CVD + no vector |
| Positive Control | CVD + rhBMP-7 (50ng/ml) |
| Ad-BMP7 | CVD + Ad-BMP7 (PN10$^{11}$) |

**Figure 4. Experimental design of the in vivo study.**

A. Photographs of the custom-manufactured step drill (left) and SLA-treated titanium dental implant (right). Scale bar = 1mm. B. The experimental timeline for the in vivo study showing the timepoints for bilateral 1st molar extractions, implant placements, and endpoints for microCT and histological analysis. C. Schematic diagram showing the dimensions of the surgically-created osseous defect and positioning of the titanium implant within the alveolar bone. D. Table showing the experimental and control treatment groups. A total of 54 rats were assigned and a total of 108 implants were placed.

Each timepoint had 12 implants placed per group with split mouth design and the surgeon was masked for the group of implants.

To quantify the regenerated bone volume around the implants and measure the bone mineral density (BMD), micro CT analysis was performed (**Figure 5**A-C, **Table 1**). In in-vivo study, a total of 108 implants which consists of 12 implants per group were analyzed. During the micro CT analysis, we found 2 implants were perforated nasal cavity at day 10. In addition, 1 implant at day 14 were perforated nasal cavity, 4 implants at day 21 were lost, and 6 implants at day 21 were placed with malposition. Thus, those samples were excluded for further analysis. Twelve samples in Control, 11 in rhBMP-7, and 11 in Ad-BMP7 at day 10, 11 in Control, 12 in rhBMP-7, 12 in Ad-BMP7 at day 14, and 9 in Control, 8 in rhBMP-7, 9 samples in Ad-BMP-7 at day 21 were analyzed for µCT and histomorphometry. At 10 d post-surgery, variable bone regeneration in the defect area was observed in all groups and increased at 14 d post-surgery, but with no differences measured among the groups (Figure 5A and B). At day 21, the rhBMP-7 treatment significantly increased the volume of regenerated bone within the defect compared to controls (Figure 5B). Ad-BMP7 gene delivery showed similar results as the rhBMP-7 protein group, with increased regeneration compared to the control although it's not significant (p=0.089) (Figure 4B and Table 1). Both the rhBMP-7 and Ad-BMP7 treatment groups demonstrated a significantly higher BMD within regenerated bone at day 21 compared to days 10 and 14. In addition, rhBMP-7 showed a significantly higher BMD compared to the Control group and was similar with respect to the regenerated bone volume (Figure 5C). The BMD in the Control group at day 21 showed significance only when compared to day 10 (Figure 5C and Table 1). Regarding tissue mineral density (TMD), the rhBMP-7 and Ad-BMP7 treatment groups showed a higher TMD at 10 days post-surgery. However, all groups showed an increasing TMD throughout the experiment (Supplementary Table S1).

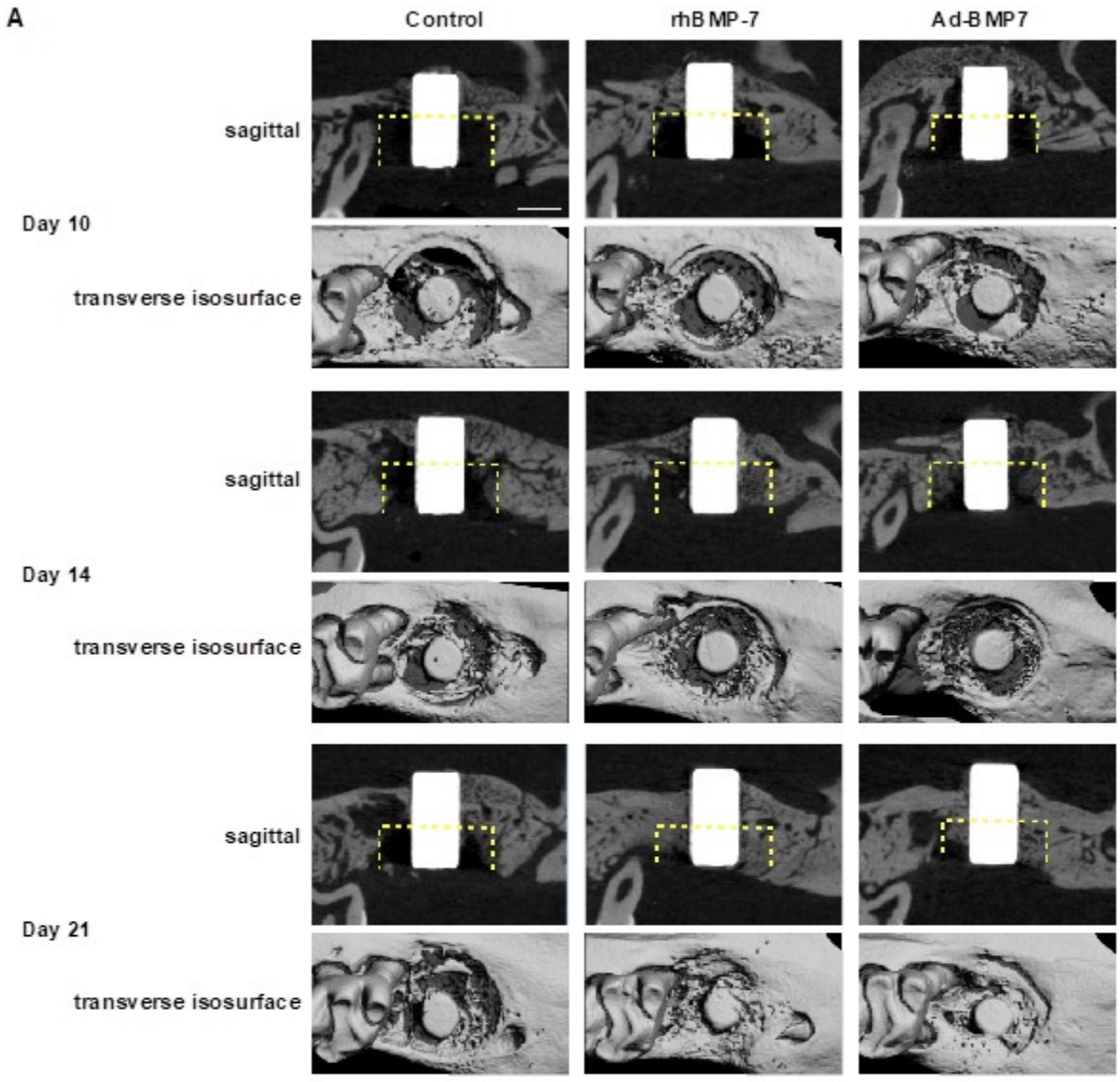


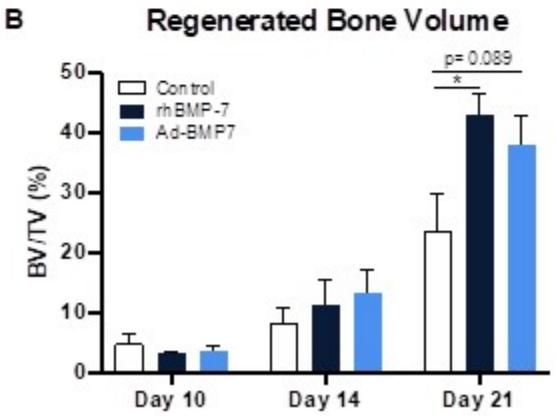


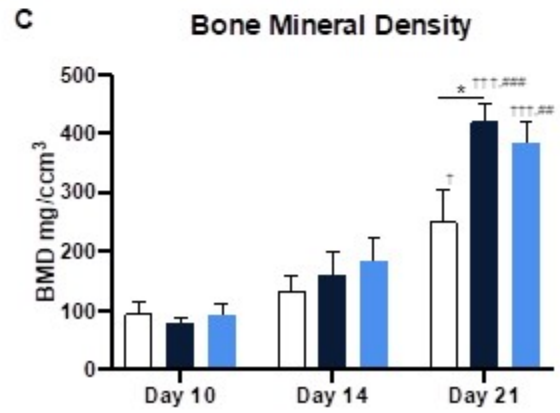

**Figure 5. Results from the microCT analysis measuring regenerated bone volume and bone mineral density within the surgically created defect.**

A. 10, 14, and 21 d sagittal images from microCT scanning (upper panels) and the corresponding 3D transverse isosurface images (lower panels) for the respective treatment groups. Yellow-dashed lines outline the region of interest for measurements. Scale bars = 1 mm. B. Statistical data showing the total bone regenerated (%) within the defect and C. bone mineral density (BMD) within the defect. Eleven or 12 samples per group at days 10 and 14, and 8 or 9 samples per group at day 21 were performed with micro CT analysis. Data are expressed as Mean ± SEM, One-way ANOVA, Dunnett's post-hoc test for regenerated bone volume and Tukey's post-hoc test were performed for bone mineral density. p= 0.0315, * p< 0.05 compared to Control in Day 21, † p< 0.05 compared to same group in Day 10, ††† p< 0.0001 compared to same group in Day 10, ## p< 0.01 compared to same group in Day 14, ### p< 0.0001 compared to same group in Day 14.

**2.4. Backscattered electron-scanning electron microscope (BSE-SEM) images confirmed significant bone regeneration within the defects in the Ad-BMP7 group**

To confirm the results from the microCT analysis, BSE-SEM analysis using undecalcified tissue sections was performed. The BSE-SEM technique produces high resolution images of bone directly surrounding the implants without producing a "halo" effect. BSE-SEM images, which are cross-sectional views from the midline of the implant, were used to measure the regenerated bone volume within the defect (**Figure 6**A, and **Figure 7**A-C). At 10 d post-surgery, regenerated bone was measured in both rhBMP-7 and Ad-BMP7 groups and the total amount of bone increased by 14 d post-surgery. At 21 d post-surgery, both the rhBMP-7 and Ad-BMP7 groups showed a significant amount of regenerated bone at approximately the same height of the implant (~1mm). In contrast, even at 21 d, the control group did not produce an equivalent amount of bone height (Figure 6A). It is noteworthy that Ad-BMP7 significantly regenerated bone volume within the defect at 21 d post-surgery compared to the control, whereas rhBMP-7 showed similar results but it was not significant when compared to the control (Figure 7A and C).

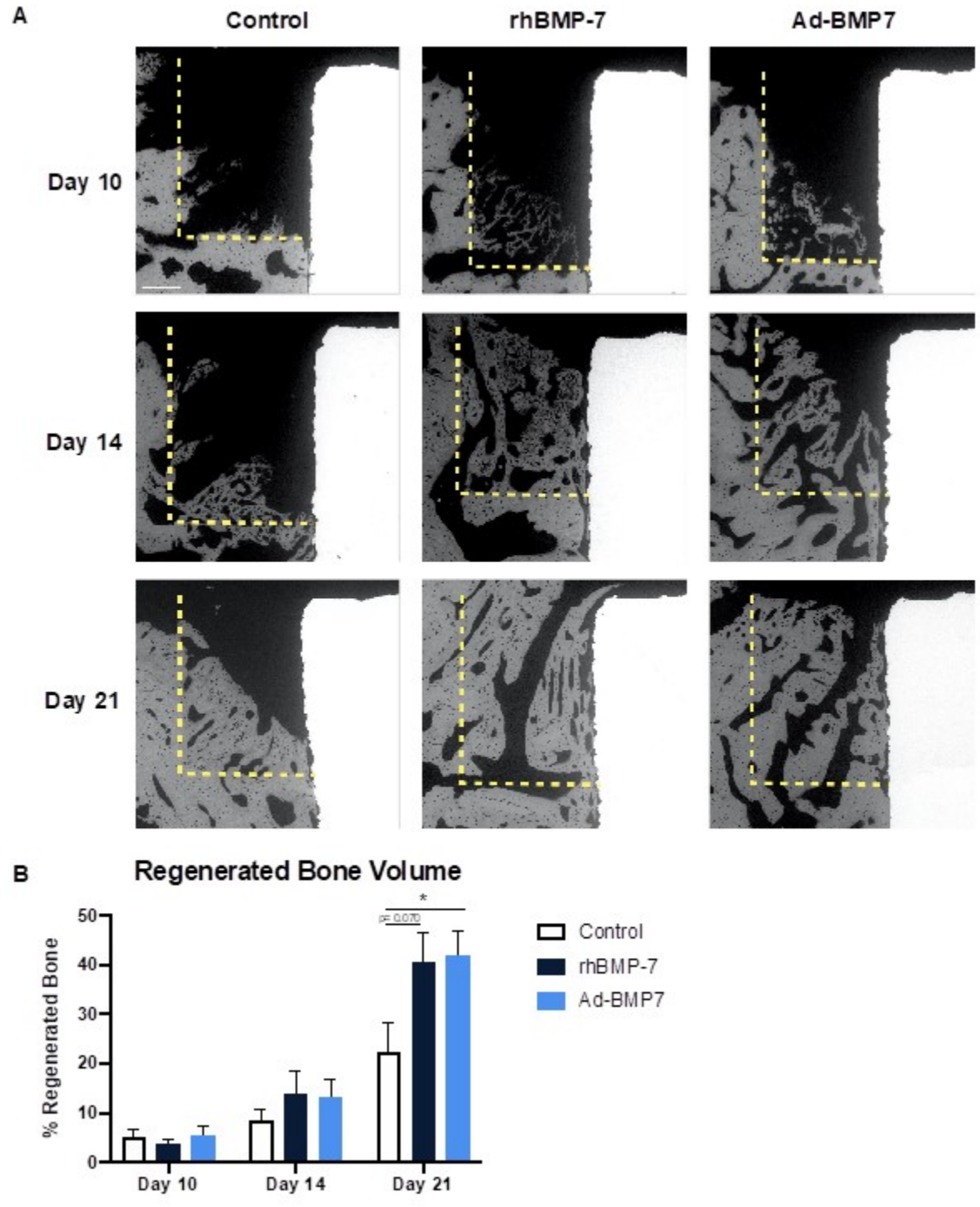


**Figure 6. Histomorphometric analysis of back-scattered electron-scanning electron microscopy (BSE-SEM) images revealed enhanced bone regeneration using CVD-BMP-7 gene delivery.**

A. Undecalcified tissue samples were embedded in MMA and sectioned, ground and polished to ~50um thickness, then subject to BSE-SEM. Representative day 10 (top), 14 (middle) and 21 (lower) images for each treatment group with the yellow-dashed line outlining the defect area created at the time of surgery. Eleven or 12 samples per group at days 10 and 14, and 8 or 9 samples per group at day 21 were performed with histological analysis. Scale bar = 200μm. B. Statistical data showing the mean values for alveolar bone regeneration (%) within the defect area for each treatment group at each time point. Data are expressed as Mean ± SEM, One-way ANOVA, and Dunnett's post-hoc test were performed. P< 0.05, * p< 0.05 compared to Control in Day 21.

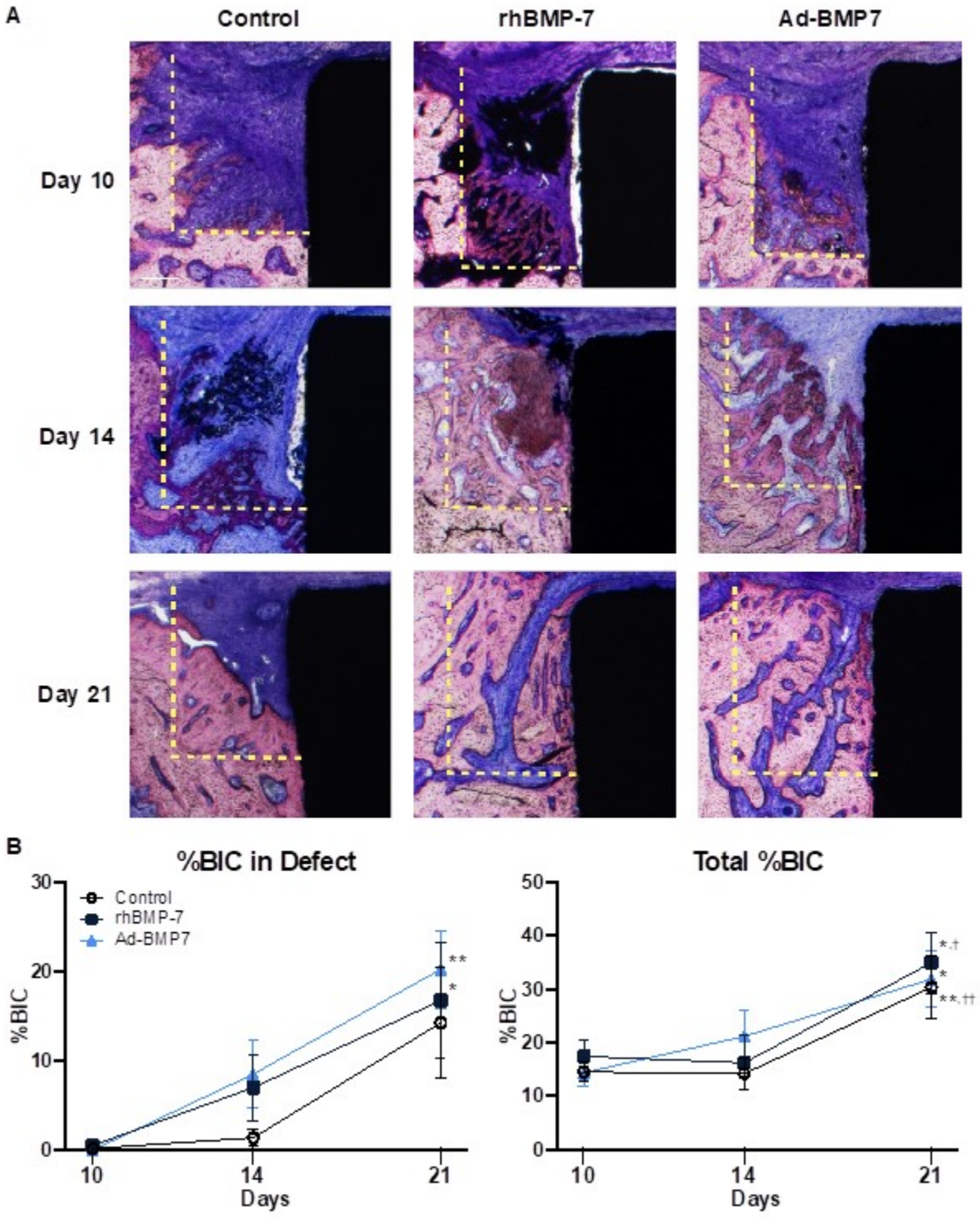

**Figure 7. Bone-to-implant contact measurements using histological sections stained with toluidine blue and basic fuchsin.**

A. The exact same tissue sections used for BS-SEM in Figure 6 were stained with toluidine blue and basic fuchsin to calculate the BIC. Representative day 10 (top), 14 (middle) and 21 (lower) images for each treatment group are shown with the yellow-dashed line outlining the defect area. Eleven or 12 samples per group at days 10 and 14, and 8 or 9 samples per group at day 21 were performed with histological analysis. Scale bar = 200μm. B. Statistical data showing the bone-to-implant contact measurements of % within the defect (left) and % of the total implant length. Data are expressed as Mean ± SEM, One-way ANOVA, and Tukey's post-hoc test were performed for bone mineral density. $p< 0.05$, * $p< 0.05$, ** $p< 0.01$ compared to same group in Day 10, † $p< 0.05$, †† $p< 0.01$ compared to same group in Day 14.

### 2.5. rhBMP-7 and Ad-BMP7 showed significant % BIC at 21 days post-surgery

To evaluate the effect of Ad-BMP-7 vectors tethered to the Ti implants on the bone to implant contact (BIC), histomorphometric analysis was performed. Histological images shown in Figure 7A are from the same sections as in the BS-SEM images (Figure 6A). Histomorphometric analysis revealed that at day 10, both Ad-BMP7 and rhBMP-7 treatment significantly increased the % BIC within the defect. Additionally, both groups showed an increase in % BIC within the defect at day 14. Regarding the total percentage of BIC, Ad-BMP7 showed an increase at day 14, but was not significantly different compared to the other groups. At day 21, all three groups showed a significantly higher % BIC compared to the day 10 values.

## Discussion

Bone repair has been well-studied within the field of regenerative medicine. With the recent advances in tissue engineering technology, hopes and expectations applying these new regenerative strategies have increased, leading to numerous studies being conducted to enhance

the key elements of regeneration, which include cells, scaffolds, and growth factors. Among the several types of growth factors, BMPs have received much attention for bone regeneration[17]. The concentrations of various BMPs in normal human plasma are reported to be less than 100 pg/ml, and it is known that the concentration of BMPs increases when fractures occur[18]. Recombinant forms of BMP, specifically BMP-2, BMP-4, and BMP-7, have been shown to improve bone regeneration in animal models[19]. Of these, rhBMP-2 and rhBMP-7 are approved for clinical use by the Food and Drug Administration (FDA)[20], and the clinically approved doses of rhBMP-2 and rhBMP-7 are in the milligram range.[21]. The osteoinductive potential of rhBMPs has been proven in both *in vitro* and preclinical studies, however, clinical applications have not achieved widespread clinical adoption in dental medicine due to economic feasibility [22]. It has been suggested that high dosage administration of rhBMP due to a short half-life is one of the main causes of reported adverse events[21a]. Therefore, new studies for the controlled release of BMPs have been introduced to address this concern.

Adenoviral vectors are commonly used for gene delivery due to their specific advantages, including a high transduction efficiency on both non-dividing and dividing cells, epichromosomal persistence in the host cell, and inability to be incorporated into the host cell genome[23]. Although adenoviral vector DNA can be immunogenic, its transfection is characterized by a transient and high expression of specific genes[24]. This feature is particularly relevant for the purpose of regenerating bone at localized oral defects around the implant[25]. In this study, we used CVD technology to bind a BMP-encoding gene onto titanium implant surfaces. Based on the previous study [12], the binding efficacy is nearly 100%, within a wide range from $10^8$ to $10^{11}$ PN. We used a concentration above saturation (10 μg/ml of antibody) so that all functional groups are blocked and bound with antibody. BMP-7 protein was measurable at two Ad-BMP7 particle numbers, $10^{11}$ and $10^{12}$, showing production at a high concentration of approximately 50 ng/ml of BMP-7 on day 7 (Figure 2A). The pattern of cell morphology was divided into two groups; a non-CVD treatment group (no treatment and rhBMP-7) and a CVD group (CVD + empty vector and CVD + Ad-BMP7). Results showed slightly elongated cells and were seemingly less in number for the CVD group (Figure 2A). We believe that the pattern of cellular morphology was affected by actin cytoskeletal reorganization by adenovirus endocytosis[26], but this did not have a significant impact on cell proliferation or differentiation

(Figure 2B and 3). The quantitative real-time PCR and ALP assay data showed that CVD + Ad-BMP7 exhibited osteogenic responses that were equivalent to or slightly higher than that of rhBMP-7 (Figure 3). Thus, Ad-BMP7 tethered on titanium resulted in a strong enhancement for osteogenic differentiation of preosteoblasts in vitro.

From the in vivo experimental data, it is especially noteworthy that Ad-BMP7 enhanced bone regeneration, bone mineral density, and % BIC around the implants similar to local delivery with rhBMP-7 protein. This was observed at 14 d post-surgery with significant differences measured at day 21. These results appear to be a milestone for improved development of implant surface properties, since current clinical dentistry often requires invasive surgeries to regenerate bone prior to the implant placement given that there are no bioactive implants clinically available. Wikejö et al. reported the effect of rhBMP-2 and rhBMP-7 coating on implants[27]. Using a supraalveolar peri-implant defect model in canines, prominent osteogenesis was observed around the implants. However, the % BIC and bone density of the newly formed bone was less than the control. Another study investigating implant coating using recombinant human growth/differentiation factor-5 (rhGDF-5) yielded stable results without any cases of seroma formation or implant dislocation[28]. However, bone regeneration using rhGDF-5 seemed to be less than with rhBMP-2 or rhBMP-7, and lower bone density and %BIC were found compared to controls[29]. Although the experimental design parameters such as animal species, implant design, and defect morphology were different from our study, we have shown not only significantly higher bone regeneration, but also increased bone mineral density, and % BIC using Ad-BMP-7 compared to the control. In addition, there were no post-surgical complications such as seroma or dislocation of implants among the groups.

Currently, there remains a need for dose or carrier optimization of rhBMPs or other growth factor proteins used for effective treatments[30]. In this regard, the CVD coating and gene delivery technology used in this study is a highly innovative and beneficial method. In a study of peri-implant defects using Ad-BMP7 and collagen gel, in vivo bioluminescence imaging showed that Ad-BMP7 maintained higher transgene expression within the target site for 10 d, returning to baseline by 35 d[8a]. The use of a collagen gel can help maintain local gene expression for a period of time[8a], but systemic transmission within the bloodstream may occur[9a]. In the present study, Ad-BMP7 tethered to the titanium implant using CVD resulted in significant bone regeneration and high % BIC around

the implant (Figure 5-7) with approximately 1/3 of the amount of the Ad-BMP7 used compared to a previous collagen gel study[8a]. The reason for this result may be due to CVD demonstrating a strong capacity for adenovirus capture on the surface of the implant and promoting viral transfection, while suppressing the systemic transmission of adenovirus vector. In addition, we were able to achieve comparable regenerative results as compared to conventional protein delivery using a supraphysiological concentration of rhBMP-7 (Figure 5-6).

For optimal dental implant treatment, it is necessary to have sufficient bone volume and appropriate bone quality in order to place the implants in the exact location and maintain stability. This study suggests that CVD-coated implants could be used as an effective implant treatment even in areas with insufficient bone volume. Hao et al. reported that CVD can be applied to several biomaterials, which can potentially be combined together with 3D printed materials and Ad-BMP7 and Ad-PDGF transfected into human periodontal ligament cells (hPDL)[6]. Our in-vitro study revealed that CVD-tethered adenovirus can efficiently transfect genes into various cell types, such as oral keratinocytes, hPDL, human gingival fibroblasts, and bone marrow stem cells (Figure S1, supplemental information). Moreover, a CVD coated micropattern-scaffold effectively transfected adenovirus within periodontal tissue resulting in enhanced periodontal regeneration[31]. Further improvements have been made to CVD technology itself, with degradable polymer coatings being developed[32]. Unlike conventional CVD monomer coatings, CVD polymers with ester groups in the main chain can be degraded and absorbed in vivo, therefore it has great potential on biomaterials used for tissue regeneration. As such, CVD coating with Ad-BMP7 may be safe and effective to use in vivo. Since this adenovirus vector is replication-deficient, it cannot replicate or proliferate post-transduction, and the virus will thereby 'disappear' after internalization. Chang et al, showed acceptable biosafety profiles using this adenovirus vector in vivo[9a]. Since our adenovirus vectors were tethered to the titanium surface and are not released from material surface compared to collagen gel, we assume our adenovirus immobilization using CVD is safer than collagen gel delivery. Furthermore, our present study also showed no progressive swelling or symptoms noted. Our method of using CVD to polymer coat implants and deliver Ad-BMP7 can be effective to stimulate bone regeneration directly surrounding the implant enabling a reduction of traditional bone regeneration procedures and will help satisfy the increased demand for implant dentistry. We

believe this innovative CVD coating and gene delivery methodology can be applied to dental implant reconstruction, resulting in a more ideal alveolar bone tissue regeneration with better targeting of growth factors. The application of these tailor-made regenerative therapies specific to the individual and disease site may not be far off in the future.



## 3. Conclusion

These results propose that using chemical vapor deposition to immobilize a BMP-7 gene-expressing adenovirus onto titanium surfaces enhances osteoblast differentiation and osteogenic potential in vitro, and subsequently can increase the alveolar bone regeneration and % BIC similar to that of using high doses of locally-applied rhBMP-7 in vivo. The use of chemically-immobilized gene therapy vectors onto implant surfaces allows for targeted gene transfer at the implant-cellular interface without the need for high doses of growth factors using traditional protein delivery. This approach offers potential as a treatment modality in the targeting of cells to produce regenerative molecules and potentially improve the biosafety of such approaches for local drug delivery.

## 4. Experimental Section/Methods

*Titanium disc/implant manufacture and CVD coating*: Titanium discs measuring 12 mm in diameter and 1 mm in thickness, were manufactured by ELOS Medtech (Gorlose, Denmark). The titanium disc surface was machined and smooth surface. The discs were coated with a layer of amine-reactive polymer using a custom-built CVD system as previously reported[6]. Sand-blasted, Large grit, Acid-etched (SLA) press-fit implants (kindly donated by Straumann, Switzerland), with a diameter of 1.0 mm and 2.0 mm in length were used. (Figure 4A). Briefly, a thin layer of polymer film containing pentafluorophenol (PFP)-ester groups was coated on the implant surface via CVD polymerization. X-ray photoelectron spectroscopy (XPS) and immunofluorescence were used to verify the presence of polymer and binding of anti-adenovirus antibody on the polymer-coated disc surface. The thickness of the coating was measured by an elipsometer (EP3 Nanofilm, Accurion, Germany).

*Adenoviral vector gene delivery*: Replication-deficient adenoviral vector (Ad) encoding BMP7 was generated by the University of Michigan Vector Core lab. The viral titer was approximately 4.0 x $10^{12}$ PN/ml and the virus concentration used for conjugation to the anti-adenovirus antibody was $10^{11}$ and $10^{12}$ PN/ml. CVD coated titanium discs or implants were incubated overnight at 4˚C in PBS containing 10 µg/ml goat anti-adenovirus antibody (AbD Serotec, Oxford, UK). Following 3-5 washes with PBS, the titanium discs/implants were incubated in a $10^{11}$ or $10^{12}$ PN/ml Ad-BMP7 solution for 4h and then washed again to remove any unbound virus particles. Coated samples were handled aseptically for all steps following CVD coating. No contamination or inflammatory events were observed throughout the in vitro experiment.

*Cell culture*: MC3T3-E1 mouse pre-osteoblast cells were cultured in α-Minimum Essential Medium Eagle (α-MEM) with 10% fetal bovine serum (FBS) containing 100 U/mL penicillin and 100 µg/mL streptomycin in a 37˚C incubator with 95% air, 5% $CO_2$, and 100% relative humidity. MC3T3-E1 cells were plated at 3x$10^4$ cells on the discs, which were placed in multi-well tissue culture plates (Figure 1A) and cultured in osteogenic media to induce osteoblastogenesis. Three samples per group were used. The osteogenic medium was prepared by adding 50 µg/ml ascorbic acid and 10 mM β-glycerophosphate and the media was changed every three to four days (Day 0, 3, 6, 9 and 13). For the positive control samples, rhBMP7 (50 ng/ml) was freshly added to the medium at every medium change (Figure 1B). Cells and cell culture supernatants were collected and stored at -80 ˚C for subsequent analysis at the time points shown (Figure 1B).

*Experimental groups in in-vitro study*: Five groups were tested in this study; no treatment (negative control), rhBMP-7 (50 ng/ml, positive control), CVD + empty vector ($10^{11}$ PN) and CVD+Ad-BMP7 ($10^{11}$ and $10^{12}$ PN), (Figure 1C).

*Cell attachment*: Twenty-four hours after cell seeding, disc-adherent cells were fixed in 4% formaldehyde for 10 minutes, followed by a quick rinse in PBS and incubation in 0.25% Triton-X for 5 min. Fixed cells were labeled with Alexa Fluor 488 phalloidin (Invitrogen, Carlsbad, CA, USA) and mounted in ProLong® Gold Antifade Mountant with 4, 6-diamidino-2-phenylindole (DAPI; Invitrogen, Carlsbad, CA, USA) for detection of cytoskeleton and nucleus, respectively. Alexa Fluor 488 phalloidin was diluted 1:20 in PBS and added to the cells. After 15 min of incubation at room temperature (RT)

in the dark, cells were rinsed once with PBS. One drop of ProLong® Gold Antifade Mountant was applied to the specimen and cover slide mounted specimen was examined. Fluorescence was visualized by CLSM.

*Cell proliferation assay (MTT assay):* Cellular proliferation was evaluated at designated days using a Vybrant® MTT Cell Proliferation Assay Kit (Thermo Fisher Scientific, USA) according to the manufacturer's instructions. Briefly, cells were labelled with MTT solution and centrifuged. The medium was removed and cells were incubated in DMSO at 37°C for 10 min. The results were evaluated using a spectrophotometer at 540 nm wavelength.

*ELISA*: The cell culture supernatants were collected at 1, 4, 7, 10, and 14 days (Figure 1B) and stored at -80°C, and used for the detection of soluble BMP7 protein using Quantikine® enzyme-linked immunosorbent assay (ELISA) kits from R&D Systems (Minneapolis, MN, USA) according to the manufacturer's instructions. Reading of the results was performed at 492 nm wavelength.

*Real-time PCR analysis*: Cells cultured on the Ti discs (N= 3/group) were harvested at 1, 4, 7, 10, and 14 d (Figure 1B). Total RNA extraction was performed using the RNeasy kit (Qiagen, Valencia, CA). The quantity and quality of the total RNA was evaluated using a NanoDrop. All samples representing an appropriate A260/280 and A260/A230 ratios above 2.0 were considered for analysis. 200 ng total RNA was used for cDNA synthesis (PrimeScript RT reagent Kit, Takara.bio inc, Shiga, Japan). SYBR green reagents (PowerUp SYBR Green master mix, Applied Biosystems, Foster City, CA, USA) were used for detection of markers of osteogenic differentiation including Collagen Type I (*ColA1*), Runt Related Transcription Factor 2 (*Runx2*), Alkaline Phosphatase (*Alp*), and Osteocalcin (*Ocn*) as well as a positive control (*Gapdh*). The primers used are listed in supplementary Table 2. An ABI PRISM 7700 sequence detector (Applied Biosystems) was used with the following settings: activation $95^0$ C, 2s; denaturation $95^0$C, 15s and annealing/extension $60^0$C, 30s. Each reaction was performed in technical duplicates and the mean of three independent biological replicates was calculated and the relative expression levels were normalized to glyceraldehyde-3-phosphate dehydrogenase (*Gapdh*) and calculated using the $2^{-\Delta\Delta CT}$ method.

*Alkaline Phosphatase activity assay*: The cell culture supernatant was collected at 1, 4, 7, 10, and 14 d (Figure 1B). An ALP activity assay was performed using the colorimetric Alkaline

Phosphatase Activity Kit from Abcam (Cambridge, MA, USA) according to the manufacturer's protocol and the absorbance was measured at OD 405 nm.

*Customized step drill and press-fit mini implants specialized for rats*: To achieve a consistent bony defect as well as placing of the implants, a customized step drill (Richard Micro-Tool, MA, USA) was designed (Figure 4A). The bony defect diameter was 2.2 mm and the depth was 1.0 mm at the coronal half of the press-fit implant. The SLA titanium implants (Straumann) were 0.95 mm in diameter and 2.0 mm in length.

*Animals, tooth extraction, and implant placement*: All animal procedures were performed with approval from the University of Michigan Institutional Animal Care and Use Committee according to the ARRIVE guidelines for preclinical studies (approved protocol ID: PRO00008696). A total of 54, 5-week-old Sprague Dawley male rats (Charles River Laboratories, MA) were acclimatized. Preemptive analgesic (Carprofen, 5 mg/kg body weight) was subcutaneously administered 1d before surgery. Isoflurane was used to anesthetize the rats and maxillary 1st molars were extracted bilaterally. After a 6 week healing period, the standardized defects were created. A surgeon, masked to the treatments, placed CVD coated implants with either no vector (Control), or with $10^{11}$ PN of Adenovirus encoding BMP-7 (Ad-BMP7) bilaterally. Each group has a total of 12 implants were randomly placed with a split mouth design, per each time point. As a positive control, 30 µg/ml recombinant human BMP-7 protein in collagen-gel (2.6%) were applied into the created defect with untreated implants (rhBMP-7). Then the flap was re-positioned and tissue glue (PeriAcryl, n-Butyl Cyanoacrylate; GluStitch Inc., Delta, B.C., Canada) was applied to close the wound. Subcutaneous administration of analgesic (carprofen, 5 mg/kg) was administered within 24 h post-surgery as well as a 5% glucose water solution supplemented with ampicillin (268 mg/l) for 48 h post-surgery for prevention of infection.

*Preparation for µCT scanning*: Rats were euthanized with an overdose Inhalation of $CO_2$ at days 10, 14, and 21 post-surgery and the maxillae were harvested. The specimens were fixed with 10% formalin for 2 d, then placed in a 34 mm diameter specimen holder and scanned using a microCT system (µCT100 Scanco Medical, Bassersdorf, Switzerland). Scan settings were: voxel size 18 µm, 90 kVp, 44 µA, 0.5 mm AL filter, and integration time 1000 ms. For acquisition of the µCT

images, all specimens were properly oriented along the sagittal plane. Titration of the halo effect was performed and the regenerated bone volume within the bony defect was calculated and quantified by a well-experienced examiner (SM) in a blinded manner using Scanco software.

*Histologic and histomorphometric experiments*: Undecalcified sections were prepared for histology and histomorphometric analyses by the Michigan Integrative Musculoskeletal Health Core Center. Briefly, the samples were dehydrated in step gradients of alcohol, infiltrated, and embedded in methyl methacrylate (MMA) by routine histological methods. One or two cross-sectional sections of approximately 50-mm thickness was cut along each implant's long axis using a diamond saw at the central portion of each implant (Isomet Low Speed Saw, BUEHLER, USA). Each specimen was attached to a plastic slide, ground down to less than 20 μm with an Ecomet 300 Pro Grinder-Polisher (Buehler, USA), and polished well. After obtaining histological sections, photo microscopic images including unstained images and calcein-labeling fluorescence images were captured with a Nikon Eclipse E800 microscope (Nikon Inc., Melville, NY, USA) with a SPOT-2 camera (Diagnostics Instruments, Inc., Sterling Heights, MI, USA). For the histomorphometric analysis, we used NIS-Elements software version BR-3.2 (Nikon Instruments, Melville, NY, USA). Then, back scattered electron (BSE) images were taken using a TESCAN MIRA3 FEG SEM (TESCAN ORSAY HOLDING, Kohoutovice, Czech Republic) at the Michigan Center for Materials Characterization. To obtain clear BSE-SEM images of bone and implant, the samples were imaged under low vacuum mode conditions with the electron beam set to 10.0 kV and beam intensity at 15.0. After obtaining BSE-SEM, the sections were stained with toluidine blue and basic fuchsin per previous protocol with slight modification. Briefly, the sections were placed in 0.1% formic acid for 5 mins, quickly rinsed with distilled water (DW), dipped into 70% ethanol for 15 mins, and stained with 1% toluidine blue for 5 mins. After rinsing with DW, sections were dipped in 70% ethanol for 1 min, and 1% basic fuchsin for 1 min., rinsed again with DW, dehydrated in step gradients of alcohol, and dried. After obtaining stained sections, histological images were again taken with the Nikon Eclipse E800 microscope, a SPOT-2, and NIS-Elements software version BR-3.2. Prior to histomorphometry, all image data were blinded prior to analysis. To minimize errors in histomorphometry analysis, experienced examiners (S. M. and N. K.) were confirmed with high intra-rater reliability (0.98 ± 0.02) and high inter-rater reliability (0.96 ± 0.04). Quantitative analyses were performed using Adobe Photoshop CC 2021

software (Adobe, CA, USA) for regenerated bone area measurements and Adobe Illustrator CC 2021 software (Adobe, CA, USA) for curved line measurements (i.e., implant outline in sections and BIC portion).

*Statistical Analysis*: All data were analyzed with using Prism 8 software (GraphPad Software, CA, USA) and SPSS (version 25.0.0.0., SPSS, Inc., IL, USA). Data was evaluated with Shapiro-Wilk Test for their normalization. In in-vitro data, 3 Discs/group were used and all samples were run in duplicate, and each experiment was performed three times. In in-vivo study, a total of 108 implants which consists of 12 implants per group were analyzed. The samples which had malpositioned or lost implants were excluded for further microCT and histological analysis, thus 11 or 12 samples per group at days 10 and 14, 8 or 9 samples per group at day 21 were used for both analysis for µCT and histomorphometry. The data presented as the mean ± standard deviation (SD) in in-vitro, and the mean ± standard error of means (SEM) in in-vivo. Comparison among multiple groups were performed with one-way analysis of variance (ANOVA) followed by post-hoc test of Tukey, or Dunnett. For the intra-rater and the inter-rater reliability tests and Chi-square test, SPSS statistical software was used to calculate (version 25.0.0.0., SPSS, Inc., IL, USA). A value of $p < 0.05$ was considered statistically significant.

**Supporting Information**

Supporting Information is available from the Wiley Online Library or from the author.

**Acknowledgements**

The authors thank Michelle Lynch in the University of Michigan School of Dentistry MicroCT core, funded in part by NIH/NCRR S10RR026475-01, for technical support with micro CT analysis. The authors acknowledge the financial support of the University of Michigan College of Engineering and NSF grant #DMR-1625671, and thank Nancy Senabulya Muyanja and Bobby Kerns for their technical support from the Michigan Center for Materials Characterization. The authors also greatly appreciate Emma Snyder-White and Carol Whitinger in the Orthopaedic Research Laboratories Histology Core, University of Michigan Medical School for their supervision during histology.

Research reported in this publication was also supported by the National Institute of Arthritis and Musculoskeletal and Skin Diseases of the National Institutes of Health under Award Number P30 AR069620. SM and YDC were supported by the Osteology Foundation, FK was funded by the ITI Foundation. Shogo Maekawa and Young-Dan Cho contributed equally to this work.

Received: ((will be filled in by the editorial staff))

Revised: ((will be filled in by the editorial staff))

Published online: ((will be filled in by the editorial staff))



References

1 a) Branemark, P. I., Adell, R., Breine, U., Hansson, B. O., Lindstrom, J.Ohlsson, A., *Scand J Plast Reconstr Surg* **(1969)**, 3, 10.3109/02844316909036699; b) Branemark, P. I., Svensson, B.van Steenberghe, D., *Clin Oral Implants Res* **(1995)**, 6, 10.1034/j.1600-0501.1995.060405.x.

2 Fillion, M., Aubazac, D., Bessadet, M., Allegre, M.Nicolas, E., *Health Qual Life Outcomes* **(2013)**, 11, 10.1186/1477-7525-11-197.

3 a) Kontis, V., Bennett, J. E., Mathers, C. D., Li, G., Foreman, K.Ezzati, M., *Lancet* **(2017)**, 389, 10.1016/S0140-6736(16)32381-9; b) GBD 2017 Disease and Injury Incidence and Prevalence Collaborators, *Lancet* **(2018)**, 392, 10.1016/S0140-6736(18)32279-7.

4 Larsson, L., Decker, A. M., Nibali, L., Pilipchuk, S. P., Berglundh, T.Giannobile, W. V., *J Dent Res* **(2016)**, 95, 10.1177/0022034515618887.

5 Zhang, Y., Song, J., Shi, B., Wang, Y., Chen, X., Huang, C., Yang, X., Xu, D., Cheng, X.Chen, X., *Biomaterials* **(2007)**, 28, 10.1016/j.biomaterials.2007.07.009.

6 Hao, J., Cheng, K. C., Kruger, L. G., Larsson, L., Sugai, J. V., Lahann, J.Giannobile, W. V., *Adv Mater* **(2016)**, 28, 10.1002/adma.201600027.

7 a) Hackett, N. R., El Sawy, T., Lee, L. Y., Silva, I., O'Leary, J., Rosengart, T. K.Crystal, R. G., *Mol Ther* **(2000)**, 2, 10.1006/mthe.2000.0203; b) Manickan, E., Smith, J. S., Tian, J., Eggerman, T. L., Lozier, J. N., Muller, J.Byrnes, A. P., *Mol Ther* **(2006)**, 13, 10.1016/j.ymthe.2005.08.007.

8 a) Dunn, C. A., Jin, Q., Taba, M., Jr., Franceschi, R. T., Bruce Rutherford, R.Giannobile, W. V., *Mol Ther* **(2005)**, 11, 10.1016/j.ymthe.2004.10.005; b) Jin, Q. M., Anusaksathien, O., Webb,

S. A., Rutherford, R. B.Giannobile, W. V., *J Periodontol* **(2003)**, 74, 10.1902/jop.2003.74.2.202.

9 a) Chang, P. C., Cirelli, J. A., Jin, Q., Seol, Y. J., Sugai, J. V., D'Silva, N. J., Danciu, T. E., Chandler, L. A., Sosnowski, B. A.Giannobile, W. V., *Hum Gene Ther* **(2009)**, 20, 10.1089/hum.2008.114; b) Gu, D. L., Nguyen, T., Gonzalez, A. M., Printz, M. A., Pierce, G. F., Sosnowski, B. A., Phillips, M. L.Chandler, L. A., *Mol. Ther.* **(2004)**, 9, 10.1016/j.ymthe.2004.02.018.

10 a) Chen, H. Y., Elkasabi, Y.Lahann, J., *J. Am. Chem. Soc.* **(2006)**, 128, 10.1021/ja057082h; b) Hu, W. W., Elkasabi, Y., Chen, H. Y., Zhang, Y., Lahann, J., Hollister, S. J.Krebsbach, P. H., *Biomaterials* **(2009)**, 30, 10.1016/j.biomaterials.2009.06.041; c) Chen, H. Y.Lahann, J., *Langmuir* **(2011)**, 27, 10.1021/la101623n.

11 Lahann, J., Choi, I. S., Lee, J., Jensen, K. F.Langer, R., *Angew Chem Int Ed Engl* **(2001)**, 40, 10.1002/1521-3773(20010903)40:17<3166::AID-ANIE3166>3.0.CO;2-#.

12 Zhang, Y., Deng, X., Scheller, E. L., Kwon, T. G., Lahann, J., Franceschi, R. T.Krebsbach, P. H., *Biomaterials* **(2010)**, 31, 10.1016/j.biomaterials.2010.01.029.

13 Amarasekara, D. S., Kim, S.Rho, J., *Int J Mol Sci* **(2021)**, 22, 10.3390/ijms22062851.

14 Rutkovskiy, A., Stenslokken, K. O.Vaage, I. J., *Med Sci Monit Basic* **(2016)**, 22, 10.12659/Msmbr.901142.

15 Huang, W., Yang, S., Shao, J.Li, Y. P., *Front. Biosci.* **(2007)**, 12, 10.2741/2296.

16 Maruyama, Z., Yoshida, C. A., Furuichi, T., Amizuka, N., Ito, M., Fukuyama, R., Miyazaki, T., Kitaura, H., Nakamura, K., Fujita, T., Kanatani, N., Moriishi, T., Yamana, K., Liu, W., Kawaguchi, H., Nakamura, K.Komori, T., *Dev. Dyn.* **(2007)**, 236, 10.1002/dvdy.21187.

17 Chen, D., Zhao, M.Mundy, G. R., *Growth Factors* **(2004)**, 22, 10.1080/08977190412331279890.

18 Ali, A. A., Mukhtar, M. M., Shaheen, S.Mohamed, A. O., *PLoS One* **(2021)**, 16, 10.1371/journal.pone.0247472.

19 a) Notodihardjo, F. Z., Kakudo, N., Kushida, S., Suzuki, K.Kusumoto, K., *J. Craniomaxillofac. Surg.* **(2012)**, 40, 10.1016/j.jcms.2011.04.008; b) Sheikh, Z., Javaid, M. A., Hamdan, N.Hashmi, R., *Materials (Basel)* **(2015)**, 8, 10.3390/ma8041778.

20 Vukicevic, S., Oppermann, H., Verbanac, D., Jankolija, M., Popek, I., Curak, J., Brkljacic, J., Pauk, M., Erjavec, I., Francetic, I., Dumic-Cule, I., Jelic, M., Durdevic, D., Vlahovic, T., Novak, R., Kufner, V., Bordukalo Niksic, T., Kozlovic, M., Banic Tomisic, Z., Bubic-Spoljar, J., Bastalic,

I., Vikic-Topic, S., Peric, M., Pecina, M.Grgurevic, L., *Int. Orthop.* **(2014)**, 38, 10.1007/s00264-013-2201-1.

21a a) James, A. W., LaChaud, G., Shen, J., Asatrian, G., Nguyen, V., Zhang, X., Ting, K.Soo, C., *Tissue Eng Part B Rev* **(2016)**, 22, 10.1089/ten.TEB.2015.0357; b) Friedlaender, G. E., Perry, C. R., Cole, J. D., Cook, S. D., Cierny, G., Muschler, G. F., Zych, G. A., Calhoun, J. H., LaForte, A. J.Yin, S., *J Bone Joint Surg Am* **(2001)**, 83-A Suppl 1.

22 a) Fu, R., Selph, S., McDonagh, M., Peterson, K., Tiwari, A., Chou, R.Helfand, M., *Ann. Intern. Med.* **(2013)**, 158, 10.7326/0003-4819-158-12-201306180-00006; b) Simmonds, M. C., Brown, J. V., Heirs, M. K., Higgins, J. P., Mannion, R. J., Rodgers, M. A.Stewart, L. A., *Ann. Intern. Med.* **(2013)**, 158, 10.7326/0003-4819-158-12-201306180-00005; c) Hiremath, G. K., Steinmetz, M. P.Krishnaney, A. A., *Spine* **(2009)**, 34, 10.1097/BRS.0b013e31819e334a.

23 Bulcha, J. T., Wang, Y., Ma, H., Tai, P. W. L.Gao, G., *Signal Transduct Target Ther* **(2021)**, 6, 10.1038/s41392-021-00487-6.

24 Crystal, R. G., *Hum Gene Ther* **(2014)**, 25, 10.1089/hum.2013.2527.

25 Kaigler, D., Cirelli, J. A.Giannobile, W. V., *Expert Opin Drug Deliv* **(2006)**, 3, 10.1517/17425247.3.5.647.

26 a) Greber, U. F.Way, M., *Cell* **(2006)**, 124, 10.1016/j.cell.2006.02.018; b) Li, E., Stupack, D., Bokoch, G. M.Nemerow, G. R., *J. Virol.* **(1998)**, 72, 10.1128/JVI.72.11.8806-8812.1998.

27 a) Leknes, K. N., Yang, J., Qahash, M., Polimeni, G., Susin, C.Wikesjo, U. M., *Clin Oral Implants Res* **(2008)**, 19, 10.1111/j.1600-0501.2008.01567.x; b) Wikesjo, U. M., Qahash, M., Polimeni, G., Susin, C., Shanaman, R. H., Rohrer, M. D., Wozney, J. M.Hall, J., *J Clin Periodontol* **(2008)**, 35, 10.1111/j.1600-051X.2008.01321.x; c) Wikesjo, U. M., Susin, C., Qahash, M., Polimeni, G., Leknes, K. N., Shanaman, R. H., Prasad, H. S., Rohrer, M. D.Hall, J., *J Clin Periodontol* **(2006)**, 33, 10.1111/j.1600-051X.2006.00985.x; d) Susin, C., Qahash, M., Polimeni, G., Lu, P. H., Prasad, H. S., Rohrer, M. D., Hall, J.Wikesjo, U. M., *J Clin Periodontol* **(2010)**, 37, 10.1111/j.1600-051X.2010.01554.x; e) Leknes, K. N., Yang, J., Qahash, M., Polimeni, G., Susin, C.Wikesjo, U. M., *J Clin Periodontol* **(2008)**, 35, 10.1111/j.1600-051X.2008.01308.x.

28 Leknes, K. N., Yang, J., Qahash, M., Polimeni, G., Susin, C.Wikesjo, U. M., *Clin Oral Implants Res* **(2013)**, 24, 10.1111/j.1600-0501.2012.02564.x.

29 Polimeni, G., Wikesjo, U. M., Susin, C., Qahash, M., Shanaman, R. H., Prasad, H. S., Rohrer, M. D.Hall, J., *J Clin Periodontol* **(2010)**, 37, 10.1111/j.1600-051X.2010.01579.x.

30 Freitas, R. M., Spin-Neto, R., Marcantonio Junior, E., Pereira, L. A., Wikesjo, U. M.Susin, C., *Clin Implant Dent Relat Res* **(2015)**, 17 Suppl 1, 10.1111/cid.12156.

31 Pilipchuk, S. P., Fretwurst, T., Yu, N., Larsson, L., Kavanagh, N. M., Asa'ad, F., Cheng, K. C. K., Lahann, J.Giannobile, W. V., *Adv Healthc Mater* **(2018)**, 7, 10.1002/adhm.201800750.

32 Xie, F., Deng, X., Kratzer, D., Cheng, K. C., Friedmann, C., Qi, S., Solorio, L.Lahann, J., *Angew Chem Int Ed Engl* **(2017)**, 56, 10.1002/anie.201609307.

**Table 1. Statistical analysis of the microCT data showing bone volume and bone mineral density for each treatment group at each time point.**

| % BV/TV | Control | rhBMP-7 | Ad-BMP7 |
|---|---|---|---|
| Day 10 | 4.7 ± 1.6 | 3.2 ± 0.4 | 3.6 ± 0.7 |
| Day 14 | 8.1 ± 2.5 | 11.2 ± 4.2 | 13.1 ± 3.8 |
| Day 21 | 23.4 ± 6.3 | 43.0 ± 3.4* | 38.0 ± 4.8 |

| BMD mg/ccm$^3$ | Control | rhBMP-7 | Ad-BMP7 |
|---|---|---|---|
| Day 10 | 95.9 ± 20.7 | 78.8 ± 8.2 | 94.6 ± 17.8 |
| Day 14 | 133.6 ± 24.5 | 161.0 ± 38.4 | 185.5 ± 36.7 |
| Day 21 | 251.4 ± 54.3$^{\dagger}$ | 420.1 ± 29.6$^{*,\dagger\dagger\dagger,\#\#\#}$ | 383.6 ± 36.0$^{\dagger\dagger\dagger,\#\#}$ |

N = 11 or 12/group at days 10 and 14, and 8 or 9/group at day 21. * p< 0.05 compared to Control in Day 21, † p<0.05 compared to same group in Day 10, ††† p<0.0001 compared to same group in Day 10, ## p<0.01 compared to same group in Day 14, ### p<0.0001 compared to same group in Day 14.

This innovative study is the first to combine the use of CVD technology and BMP gene delivery on titanium implant surfaces as an alternative treatment option for targeted alveolar bone reconstruction and the promotion of bone regeneration in vivo.